miR-4792 regulates inflammatory responses in *Cryptococcus neoformans*-infected microglia

GUOTAI YAO[1*], XIAOLI WANG[1*], YAN WANG[1*], QING HOU[1], RUI GAO[1], YILIN WANG[1], LIANG TENG[1], WENTING LIN[1], ZHONGZHI WANG[2], YI JIN[1] and JIANGHAN CHEN[3]

[1]Department of Dermatology, Changzheng Hospital, Naval Medical University, Shanghai 200003; [2]Department of Dermatology, Shanghai Skin Disease Hospital, Tongji University School of Medicine, Shanghai 200443; [3]Department of Dermatology, Shanghai Fourth People's Hospital, School of Medicine, Tongji University, Shanghai 200434, P.R. China

Received December 25, 2020; Accepted August 16, 2021

DOI: 10.3892/ijmm.2021.5031

Abstract. Investigating the factors that influence the inflammatory response of microglial cells is crucial for understanding the pathogenesis of cryptococcal meningitis (CM). MicroRNAs (miRNAs/miRs) play an important role in inducing host defenses and activating the immune response during microbial infection; however, the regulatory mechanisms of miRNAs in cryptococcal meningitis remain poorly defined. In a previous study, the authors assessed the miRNA profiles of THP-1 (human acute monocytic leukemia cells) cells following *Cryptococcus neoformans* (*C. neoformans*) infection. In the present study, it was found that miR-4792 expression was downregulated in BV2 cells infected with *C. neoformans*, whilst that of its target gene, epidermal growth factor receptor (EGFR), was upregulated. Infected cells in which miR-4792 was overexpressed exhibited a decreased EGFR transcript expression, reduced mitogen-activated protein kinase (MAPK) signaling and a decreased secretion of inflammatory cytokines. In addition, following antifungal treatment in patients with cryptococcal meningitis, the levels of miR-4792 in the cerebrospinal fluid significantly increased, whilst the expression of EGFR significantly decreased. In addition, receiver operator characteristic analysis revealed miR-4792 (AUC_{ROC}=0.75) and EGFR (AUC_{ROC}=0.79) as potential diagnostic markers in patients with cryptococcal meningitis.

Correspondence to: Professor Jianghan Chen, Department of Dermatology, Shanghai Fourth People's Hospital, School of Medicine, Tongji University, 1279 Sanmen Road, Shanghai 200434, P.R. China
E-mail: chenjianghan@smmu.edu.cn

Professor Yi Jin, Department of Dermatology, Changzheng Hospital, Naval Medical University, 415 Fengyang Road, Shanghai 200003, P.R. China
E-mail: jinyi0425@smmu.edu.cn

*Contributed equally

Key words: miR-4792, EGFR, MAPK, inflammatory cytokines, *Cryptococcus neoformans*

Introduction

Cryptococcal meningitis (CM) is associated with mortality rates of ~15% in patients with acquired immunodeficiency syndrome (AIDS), accounting for ~181,100 related deaths per year. China and other developing countries have observed a higher impact of CM infection in non-HIV AIDS hosts with an unknown risk of susceptibility (1,2). The lung is the first organ exposed to fungal spores following inhalation. Colonization of the fungi in the host lung leads to immune activation in the absence of fungal clearance during the incubation period, which can be reactivated when the host becomes immunocompromised, leading to asymptomatic infection. Common symptoms include pulmonary disease characterized by pulmonary nodules and inflammation (3,4). In immunosuppressed individuals, the fungi spread to other organs, particularly the brain. and cryptococcal cells proliferate hematogenously to disseminate to the brain through the blood-brain barrier (BBB) (5). Ngamskulrungroj *et al* (6) previously demonstrated that, unlike *Cryptococcus gattii*, *Cryptococcus neoformans* (*C. neoformans*) exhibits a preference for the brain as opposed to the lungs as a site of infection. *C. neoformans* can survive under phagocytosis and can endure the oxidative attack of the innate immune response, which facilitates dissemination to the central nervous system (CNS) and causes meningoencephalitis (7).

Microglia are macrophages within the CNS that participate in the immunosurveillance of *C. neoformans*. The efficiency of the immune response dictates the outcome of *C. neoformans* infection, producing a disseminated disease or state of latency. The CNS is immune-privileged and isolated from peripheral organs due to separation by the BBB. Microglial activation enhances innate immune response, enhancing the phagocytosis of invasive bacteria or fungi, thus protecting neuronal cells (8,9). The assessment of the association between macrophages, innate immunity and *C. neoformans* can enhance the current understanding of the pathogenesis of CM.

MicroRNAs (miRNAs/miRs) are highly conserved small non-coding RNAs of 18-22 nucleotides (10). miRNAs regulate gene expression by binding to the 3' untranslated region (3'UTR) of mRNAs, leading to a loss of gene expression through mRNA degradation or by preventing translation. A role for miRNAs in the immune response to fungal exposure has been documented. miR-21, miR-146, miR-132, miR-155 and the let-7 family have been shown to regulate inflammatory responses following exposure to bacterial pathogens, and a range of miRNAs have been used as therapeutics for cancers and other diseases (11). The miRNA response to fungal exposure is comparable to that of inflammatory and allergic responses (12-17). miR-4792 has been shown to be downregulated in glioblastoma-infiltrating $CD14^+$ cells, in contrast to miR-4792 that is upregulated in glioma microvesicles (18-22). Epidermal growth factor receptor (EGFR) regulates epithelial tissue development and homeostasis, its dysregulation being common in lung, breast and glioblastoma tumors. In previous studies, miRNA-34a, miRNA-101-3p.1 and miRNA-223 were demonstrated to play important roles in several disease states, including gastric cancer, chronic obstructive pulmonary disease and non-small cell lung cancer through their ability to target EGFR (23-25).

Approximately 50% of patients with cryptococcal meningitis succumb to the disease within 1 year of infection due to a lack of successful therapy (26). In the absence of effective anti-fungal agents, the immune response to fungal infection is poorly defined. In the present study, the changes in miR-4792 expression following pathogen infection and the regulation of its target genes during neuroinflammation were investigated, in order to provide a novel theoretical basis and more effective approaches for antifungal therapeutics.

Materials and methods

Cells and cell culture. Given the limited availability of primary cultures, BV2 cells were used as a representative immortalized microglia cell line due to their known similarities to primary microglia cells (27,28). BV2 cells were cultured at 37˚C in 5% CO_2 in Dulbecco's modified Eagle's medium (DMEM; Gibco; Thermo Fisher Scientific, Inc.) containing 10% heat-inactivated fetal bovine serum (FBS; Omega Scientific, Inc.) and 1% penicillin/streptomycin (all from Beyotime Institute of Biotechnology). Cell densities did not exceed $5x10^5$ cells/cm^2. The BV2 and THP-1 cell lines were purchased from the Stem Cell Bank (The Cell Bank of Type Culture Collection of the Chinese Academy of Sciences).

Induction of BV2 cells. The cells were seeded at a density of $1x10^7$ cells into 6-well plates and incubated at 37˚C with *C. neoformans* ($5x10^7$ of the WM148 strain obtained from the Centre for Preservation of Medical Mycology, Shanghai, China) for 6 h at a ratio of 5:1. The cells were subsequently treated with the EGFR inhibitor (AG1478, 40 μm) (TargetMol), miR-4792 inhibitor or inhibitor negative controls, miR-4792 mimics or mimic negative controls (Guangzhou RiboBio Co., Ltd.) for 24 h as described below.

Western blot analysis. For western blot analysis, the cells incubated with WM148 were washed three times in phosphate-buffered saline (PBS) and lysed in RIPA buffer supplemented with 1 μm phenylmethylsulfonyl fluoride (PMSF; protease inhibitor). Protein samples were quantified using a BCA Protein Assay kit (Shanghai Epizyme Biomedical Technology Co., Ltd.). Equivalent amounts of protein (15 μg) from each sample were run at 10% SDS-PAGE and transferred to 0.45 μm polyvinylidene fluoride membranes (EMD Millipore). After blocking with Protein Free Rapid Blocking Buffer (1X) (Shanghai Epizyme Biomedical Technology Co., Ltd.) at room temperature for 10 min, the membranes were first incubated with the appropriate primary antibodies overnight at 4˚C. The membranes were then washed and labeled with HRP-conjugated secondary anti-rabbit or anti-mouse antibodies (1:3,000, cat. no. 7074S, or 7076S, Cell Signaling Technology, Inc.) at room temperature for 1 h. Finally, bands were visualized with enhanced chemiluminescence (ECL) kits (Beyotime Biotech Inc), and resulting digital images were analyzed using ImageJ software (version 1.8.0, National Institute of Health) to obtain the optical densities (OD) of signals. The primary antibodies used in the study included the following: Phosphorylated (phosphor/p)-EGFR monoclonal antibodies (1:200; cat. no. sc-81488, Santa Cruz Biotechnology, Inc.), EGFR monoclonal antibodies (1:100; cat. no. sc-377229, Santa Cruz Biotechnology, Inc.), CD11b rabbit monoclonal antibodies (1:1,000; cat. no. 49420, Cell Signaling Technology, Inc.), major histocompatibility complex (MHC) class II mouse monoclonal antibodies (1:1,000; cat. no. 68258, Cell Signaling Technology, Inc.), phospho-ERK1/2 rabbit monoclonal antibodies (1:2,000; cat. no. 4370, Cell Signaling Technology, Inc.), phospho-p38 rabbit monoclonal antibodies (1:1,000; cat. no. 4511, Cell Signaling Technology, Inc.), phospho-JNK rabbit monoclonal antibodies (1:1,000; cat. no. 4668, Cell Signaling Technology, Inc.), IL-1β polyclonal antibodies (1:1,000; cat. no. 16806-1-AP, ProteinTech Group, Inc.) and TNF-α rabbit polyclonal antibodies (1:1,000; cat. no. 17590-1-AP, ProteinTech Group, Inc.). β-actin (1:5,000; cat. no. 20536-1-AP, ProteinTech Group, Inc.) was used as an internal control.

Quantification of cytokine levels. The WM148-infected BV2 cells were treated with AG1478 (40 μm) for 6 h, or transfected with miR-4792 mimics and inhibitors for 24 h as described below. Following the treatments, cell culture supernatants were collected, and IL-1α, IL-12, eotaxin, granulocyte-macrophage colony stimulating factor (GM-CSF), monocyte chemoattractant protein-1 (MCP-1/CCL2) were quantified using Mouse Multi-Analyte kits (cat. no. M60009RDPD, Bio-Plex Suspension Array System; Bio-Rad Laboratories, Inc.) according to the manufacturer's instructions. Antibody arrays were performed by Wayen Biotechnology according to established protocols. Briefly, 50 μl antibody-conjugated beads were added to assay plates to which 50 μl tissue lysates, standards and blank controls were added in the dark at room temperature with rotational speed of shaker 850 rpm/min for 2 h. After washing, 50 μl biotinylated antibodies were added in the dark at room temperature with shaking at 850 rpm/min for 1 h. The plates were then washed and 50 μl of streptavidin-phycoerythrin (PE) was added in the dark at room temperature with shaking at 850 rpm/min for 30 min. The plates were then washed and read using a Bio-Plex MAGPIX Multiplex Reader

Table I. List of primers used for RT-qPCR and mimic and inhibitor sequences.

Primer/name	Sequence
Human GAPDH-F	5'-GCACCGTCAAGGCTGAGAAC-3'
Human GAPDH-R	5'-TGGTGAAGACGCCAGTGGA-3'
Human EGFR-F	5'- GCCAAGGCACGAGTAACAAGC-3'
Human EGFR -R	5'-AGGGCAATGAGGACATAACC-3'
Mouse GAPDH-F	5'-ACCCAGAAGACTGTGGATGG-3'
Mouse GAPDH-R	5'-TCTAGACGGCAGGTCAGGTC-3'
Mouse EGFR-F	5'-CTGCCAAAAGTTCCAAGATGAGG-3'
Mouse EGFR-R	5'-GGGGCACTTCTTCACACAGG-3'
Mouse U6-F	5'-CTCGCTTCGGCAGCACA-3'
Mouse U6-R	5'-AACGCTTCACGAATTTGCGT-3'
miR-4792	CGGTGAGCGCTCGCTGGC
miR-4792 mimics	5'-CGGUGAGCGCUCGCUGGC -3'
	3'-GCCAGCGAGCGCUCACCG -5'
Mimics negative control	5'-UUUGUACUACACAAAAGUACUG -3'
	3'-AAACAUGAUGUGUUUUCAUGAC-5'
miR-4792 inhibitor	GCCAGCGAGCGCUCACCG
Inhibitor negative control	5'-CAGUACUUUUGUGUAGUACAAA -3'

F, forward; R, reverse.

(Bio-Rad Laboratories, Inc.). Bio-Plex Manager™ software (version 6.1, Bio-Rad Laboratories, Inc.) was used for data acquisition and analysis.

Reverse transcription-quantitative PCR (RT-qPCR) analysis of miR-4792 and EGFR. The cells ($1x10^5$ cells/cm^2) were seeded onto coverslips and treated with 40 μm AG1478 for 24 h following WM148 ($5x10^5$ cells/cm^2) induction. RNA was extracted at 0, 3, 6, 9 and 12 h. The expression levels of miR-4792 and EGFR in CSF were measured using miRNeasy Serum/Plasma kits (cat. no. 217184, Qiagen, Inc.) according to the manufacturer's recommendations. Total RNA was extracted using TRIzol reagent (Invitrogen; Thermo Fisher Scientific, Inc.). RNA (500 ng) was used for cDNA synthesis with reverse transcriptase (RR036B, Takara Bio, Inc.). cDNA (1 μl) was used for qPCR with GoTaq qPCR Master Mix (Promega Corporation). The reaction conditions were as follows: Hot start at 95˚C/5 min (for miRNA) or 95˚C/30 sec (for RNA); 40 cycles of 30 sec at 95˚C, 30 sec at 60˚C and 30 sec at 72˚C, and 10 min at 72˚C. Target gene expression was calculated relative to GAPDH (for RNA) or U6 (for miRNA)and values were normalized to untreated controls. The $2^{-\Delta\Delta Cq}$ method was used to quantify the relative levels of gene expression (29). The primer sequences are presented in Table I.

Transient transfection. The cells were seeded at a density of $2x10^5$ cells/plate and were transfected with miR-4792 mimics (50 nM), mimic controls (50 nM), miR-4792 inhibitor (100 nM) and inhibitor controls (100 nM) using riboFECT™ CP reagent (Guangzhou RiboBio Co., Ltd.) as per the manufacturer's recommendations. The sequences of the mimics and inhibitors are presented in Table I. Briefly, 5 μl of the miRNA mimic or 10 μl of the miRNA inhibitor were diluted with 120 μl riboFECT™ CP buffer at 37˚C for 10 min. Diluents were mixed with 12 μl of riboFECT™ CP reagent and incubated for 15 min at 37˚C. RiboFECT™ CP-miRNA mixtures were then added to the cells with 2 ml of DMEM and incubated at 37˚C for 24 h.

Luciferase reporter assay. The miR-4792 target gene, EGFR, was searched using the bioinformatics tool, miRanda (http://www.microrna.org) and TargetScan (http://www.targetscan.org). BV2 cells were exogenously transfected with either 60 nM miR-controls and 60 nM miR-4792 mimics in combination with wild-type (WT) and mutant type (mut) 3'UTR EGFR using Lipofectamine 3000 (Thermo Fisher Scientific, Inc.). At 48 h post-transfection, dual-luciferase reporter assays were performed to monitor Firefly and *Renilla* luciferase activity (Promega Corporation).

Flow cytometry. MHC II (FITC anti-mouse I-A/I-E, BioLegend, Inc.) and CD11b (APC anti-mouse/human CD11b, BioLegend, Inc.) expression were measured using a BD FACSCalibur™ (version 5.0, BD Biosciences) using flow cytometer (BD Biosciences).

Patients. CSF samples were obtained by lumbar puncture from 11 patients with CM (7 males and 4 females; age range, 16-62 years; mean age, 45 years; all HIV(-). CSF was collected before and after antifungal therapy between January, 2014 and December, 2017 at Shanghai Changzheng Hospital (patient details are presented in Table II) (29). The patient inclusion criteria were as follows: i) Clinical symptoms of CM; ii) CSF ink staining microscopic examination (+) or CSF fungal culture (+) or CSF latex agglutination test >1:8; iii) HIV test (-); iv) vital signs were stable and there are no other serious organ diseases of heart, liver, kidney, or blood system.

Table II. Clinical information of the patients with cryptococcal meningoencephalitis.

			Pre-therapy		Post-treatment	
Patient no.	Sex	Age (years)	No. of cryptococci	Antibody titer	No. of cryptococci	Antibody titer
1	Male	51	2	1:640	0	1:20
2	Male	16	0	1:40	0	1:1
3	Male	62	182	1:5120	0	1:20
4	Male	35	2	>1:5120	0	1:1
5	Male	45	10	1:5120	0	1:20
6	Male	56	42	1:80	2	1:20
7	Male	18	2	1:320	0	1:10
8	Female	40	4	1:1280	0	1:10
9	Female	49	620	1:5120	2	1:160
10	Female	60	0	1:80	0	1:10
11	Female	54	2	1:160	0	1:5

Treatment included the following: Induction treatment period: Amphotericin B 0.7-1.0 mg/kg/day intravenously guttae + flucytosine 100 mg/kg/day p.o. for at least 2 weeks; Consolidation period: Fluconazole 800 mg/day p.o. for 8-10 weeks; Maintenance treatment period: Fluconazole 200 mg/day p.o. for 6-12 months. The clinical observation period was 12 months. CSF fungal culture was negative for at least 3 consecutive times. All patients fulfilled the criteria of the Infectious Diseases Society of America (IDSA) (30). All protocols were approved by the Ethics Committee of Ethics Committee of Changzheng Hospital and written consent was obtained from all patients. The study was performed according to the declaration of Helsinki guidelines.

Statistical analysis. The majority of the experiments were performed independently at least three times and yielded similar results. Data are presented in figures as the mean ± SD using GraphPad Prism8 (GraphPad Software, Inc.). An independent two-tailed Student's t-test was used to compare two independent groups. For multiple group comparisons, one-way ANOVA was performed, and a post hoc analysis was conducted using Tukey's test. Receiver operating characteristic (ROC) curves were used to analyze the predictive value of miR-4792 and EGFR. A value $P<0.05$ was considered to indicate a statistically significant difference.

Results

miR-4792 and EGFR expression in BV2 cells following infection with C. neoformans (WM148). The preliminary data revealed that the expression of miR-4792 increased in the THP-1 cells infected with *C. neoformans* (WM148) (Fig. 1A). To further investigate the expression of miR-4792 in microglia, BV2 cells were infected with WM148 for 0, 3, 6 and 9 and 12 h and RT-qPCR was performed to detect miR-4792 expression. It was found that the expression of miR-4792 decreased over time, reaching its lowest level after 6 h (Fig. 1B), whereas the expression of EGFR gradually increased, peaking at 6 h (Fig. 1C). In a previous study, the authors demonstrated that the secretion of the inflammatory factors, TNF-α and IL-6, by microglia gradually increased over time, whereas the IL-1β levels exhibit no obvious changes (31).

EGFR is targeted by miR-4792. To further define the molecular mechanisms governing the regulatory effects of miR-4792, the bioinformatics tool, miRanda (http://www.microrna.org) and TargetScan (http://www.targetscan.org) were used to investigate novel miR-4792 targets. These analyses revealed EGFR as a miRNA target, the sequence of which was assumed to be in the 3'UTR (Fig. 2A). Additionally, western blot analysis was performed to assess the phosphorylation status of EGFR (p-EGFR) in the BV2 cells. It was found that miR-4792 overexpression significantly reduced the p-EGFR levels compared with the cells infected with WM148 for 6 h (Fig. 2B). Dual luciferase assays also confirmed EGFR as a direct target of miR-4792. The exogenous overexpression of miR-4792 significantly inhibited WT EGFR 3'UTR activity, whereas it exerted minimal effects on the mutant EGFR 3'UTR sequence (Fig. 2C). These data strongly indicate that EGFR is a direct target of miR-4792.

EGFR blockade inhibits WM148-induced microglial activation. Microglia regulate the innate immune responses of the CNS (32,33). Given that microglia are responsible for pro-inflammatory cytokine production (34), the present study examined the effects of WM148 on microglial induction. Western blot analysis and flow cytometry were performed to assess the cell surface expression of CD11b and MHC II, considered phenotypic markers of microglial activation (35). The data demonstrated that following 6 h of WM148 infection, higher levels of CD11b, MHC II and p-EGFR were observed in the infected BV2 cells (Fig. 3A). By contrast, 24 h of treatment with the EGFR inhibitor, AG1478, led to a loss of CD11b, MHC II and p-EGFR expression [Fig. 3A (bottom panels) and B] confirmed by western blot analysis and flow cytometry. Of note, miR-4792 expression was inversely associated with the EGFR levels, further highlighting EGFR as a target of miR-4792 (Fig. 3C).

Inhibition of EGFR prevents MAPK-mediated cytokine production in BV2 cells. Activated microglia stimulate

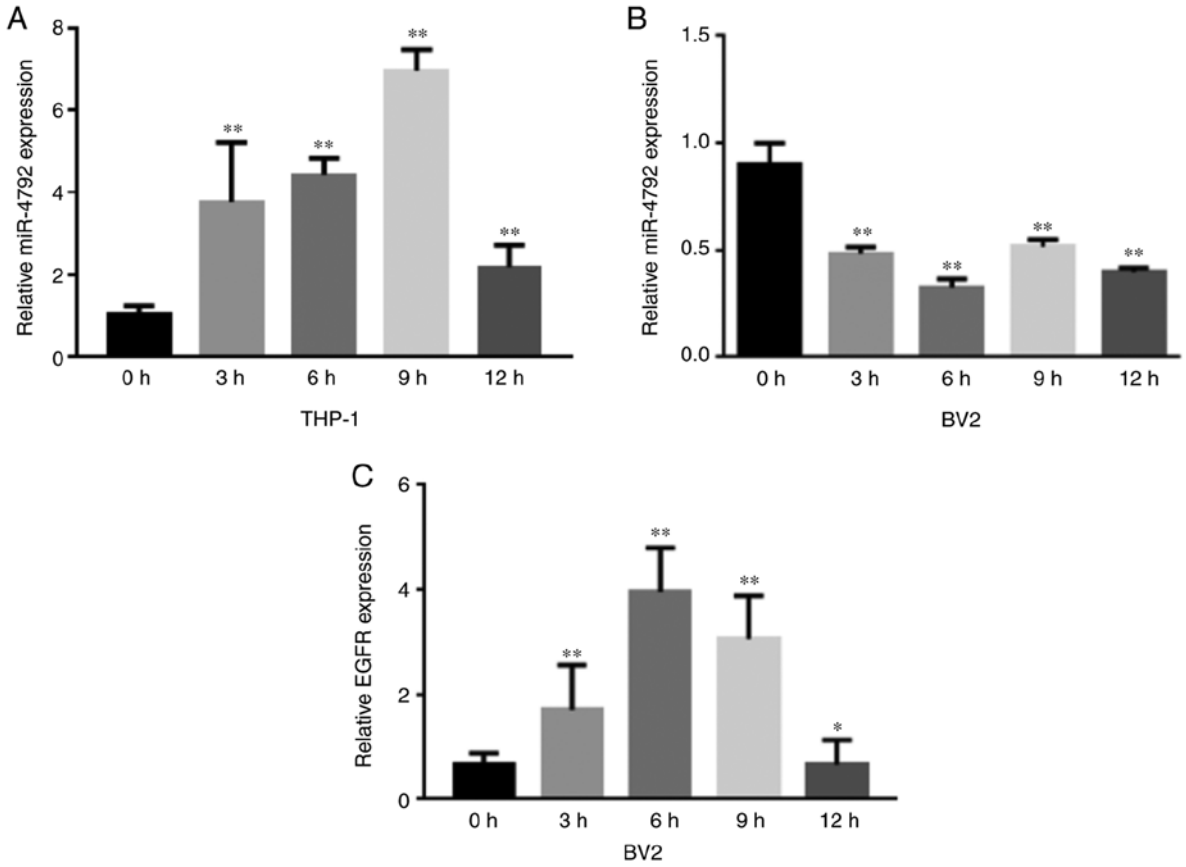

Figure 1. Expression of miR-4792 and EGFR in THP-1 cells and BV2 cells infected with *Cryptococcus neoformans* (WM148). (A) Levels of miR-4792 in THP-1 cells infected with WM148 at the indicated time points (0, 3, 6, 9 and 12 h) determined by RT-qPCR. Relative miRNA levels are shown on the ordinate. Bars present the mean values. The mean value at 0 h was set at 1. (B) miR-4792 expression in BV2 cells infected with WM148 at the indicated time points determined by RT-qPCR. Relative miRNA levels are shown on the ordinate. Bars present the mean values. The mean value at 0 h was set at 1. (C) EGFR expression in BV2 cells induced by WM148 determined by RT-qPCR. All data are expressed as the mean ± SD from three independent experiments. *P<0.05; **P<0.01, vs. 0 h.

neuronal inflammation and enhance the levels of pro-inflammatory cytokines, including IL-1β and TNF-α in the CNS (36). ERK1/2, JNK and p38 MAPK are key cell signaling cascades. MAPKs are known to enhance the production and secretion of cytokines (37-39). For example, MAPK signaling promotes the lipopolysaccharide-induced synthesis of IL-1β and TNF-α (40). MAPK is also stimulated following EGFR activation (41,42). Consistent with previous findings, the present study found that AG1478 treatment inhibited MAPK phosphorylation, leading to a loss of ERK1/2, p38 MAPK and JNK activation in WM148-infected BV2 cells. In these cells, p-ERK1/2 and p-p38 MAPK levels were significantly decreased; however, no significant differences were observed in the p-JNK levels (Fig. 4A). Similarly, AG1478 treatment inhibited both IL-1β and TNF-α production in the WM148-infected BV2 cells (Fig. 4B). The presents study then simultaneously assessed the secretion of other inflammatory factors in WM148-infected BV2 cells. The results revealed that the IL-1α, IL-12, eotaxin, GM-CSF and MCP-1/CCL2 levels decreased following AG1478 treatment compared with the control group, amongst which the expression of MCP-1/CCL2 significantly decreased (Fig. 4C).

miR-4792 regulates the EGFR/MAPK axis in BV2 cells. The present study then examined the effects of the miR-4792-mediated regulation of EGFR on ERK1/2, JNK and p38 MAPK signaling in BV2 cells infected with WM148. As shown in Figs. 2B and 5A (top and bottom panels), the levels of active p-EGFR, p-ERK1/2 and p-p38 significantly decreased in the presence of miR-4792 mimics compared with the WM148 group, whilst no significant differences in CD11b, MHC II and p-JNK levels were observed, as shown by western blot analysis. Flow cytometry revealed that the number of $CD11b^{+}$/ $MHC\ II^{+}$ cells decreased in the presence of miR-4792 mimics compared with the WM148 group, whilst no significant differences were observed in the CD11b levels (Fig. 5A, top and middle panels). The levels of the inflammatory cytokines, IL-1β and TNF-α, also decreased significantly (Fig. 5B). These findings were confirmed by RT-qPCR analysis, which revealed that the expression of miR-4792 significantly increased, and EGFR expression decreased without significance following transfection with miR-4792 mimics for 24 h. Opposite results were observed following transfection with miR-4792 inhibitors (Fig. 5C). A previous study (12) by the authors demonstrated that p-EGFR was highly expressed, whilst miR-4792 was expressed at low levels following WM148 infection (Fig. 1). Furthermore, the secretion of other inflammatory factors by WM148-infected BV2 cells was assessed. following transfection with miR-4792 mimics for 24 h, the levels of pro-inflammatory factors, including IL-1α, IL-12, eotaxin,

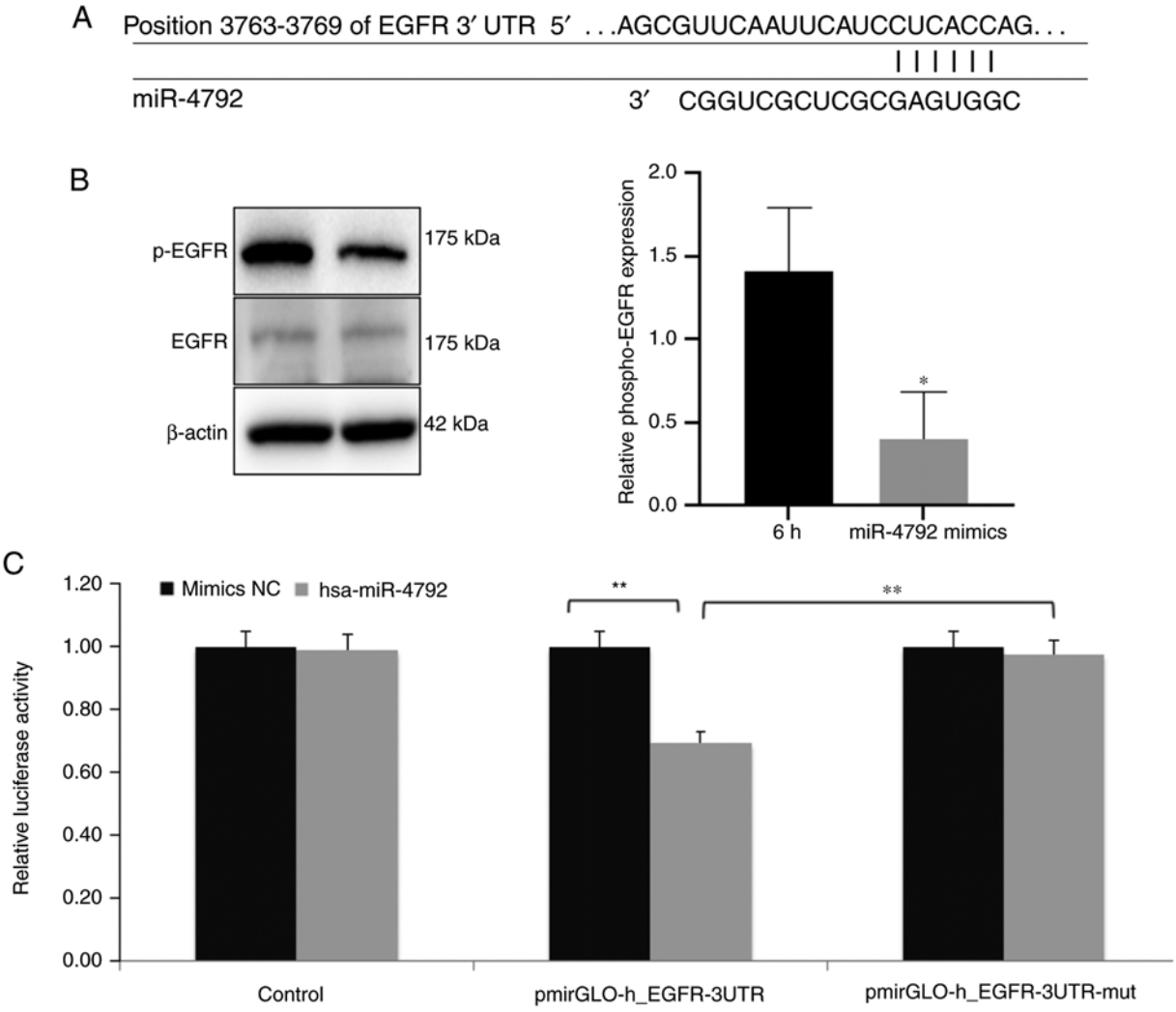

Figure 2. EGFR is a target of miR-4792. (A) Binding of miR-4792 with the 3'-UTR of EGFR was predicted using TargetScan. (B) Western blot analysis of p-EGFR levels following treatment with WM148 for 6 h and incubation with 50 nM miR-4792 mimics for 24 h. *P<0.05 compared with the control group. β-actin was used as a loading control. Protein levels were quantitated by scanning densitometry and corrected for the levels of β-actin in the same samples. Maximum levels in the controls were set as 1. Horizontal bars indicate average values. Vertical bars represent the SD. (C) Luciferase reporter assays performed to verify the binding of miR-4792 in the 3'UTR of EGFR. **P<0.01, vs. mimics NC.

GM-CSF and MCP-1/CCL2 decreased, amongst which the decrease of GM-CSF and MCP-1/CCL2 were significant (Fig. 5D). Taken together, these data highlight that in BV2 cells, miR-4792 regulates EGFR/MAPK signaling following WM148 infection and partially alleviates MAPK-mediated inflammatory responses, thus affecting the production of pro-inflammatory factors following WM148 infection.

Expression of miR-4792 in patients with CM before and after treatment. CSF was collected from patients with CM before and after regular antifungal treatment. The results revealed that the expression of miR-4792 in the CSF significantly increased following treatment (Fig. 6A). ROC curve analysis revealed an area under the curve (AUC) value of 0.75 (95% CI, 0.54-0.96) (Fig. 6C). The expression of EGFR in the CSF also significantly decreased following treatment (Fig. 6B). ROC curve analysis revealed AUCs of 0.79 (95% CI, 0.6-0.98) (Fig. 6D). These data confirmed the reciprocal association between miR-4792 and EGFR *in vivo* during fungal infection and demonstrated that the CSF levels of miR-4792, highlighting EGFR as a useful biomarker when assessing the treatment efficacy of patients with CM. Fig. 6E showed the proposed model of the regulatory and functional role for miR-4792 and EGFR in the process of *C. neoformans* infecting BV2 cells.

Discussion

Cryptococcosis is a life-threatening fungal infection, the common clinical manifestation of which is CM. The time from onset to diagnosis is relatively long, with an average of 172.9 days, and an observed mortality of 57.1% (43). CM diagnostics have rapidly improved over the past 10 years due to advancements being made in point-of-care testing that are highly specific, sensitive, accurate and capable of data production within 10 min of test initiation (https://www.immy.com/crag; https://www.biosynex.com/flyers/pro/mycologie/en/cryptops.pdf). Despite these diagnostic advances, the discovery of effective anti-fungal agents has stalled. The results of the present study provide a perspective and theoretical basis for the control of CNS inflammation following

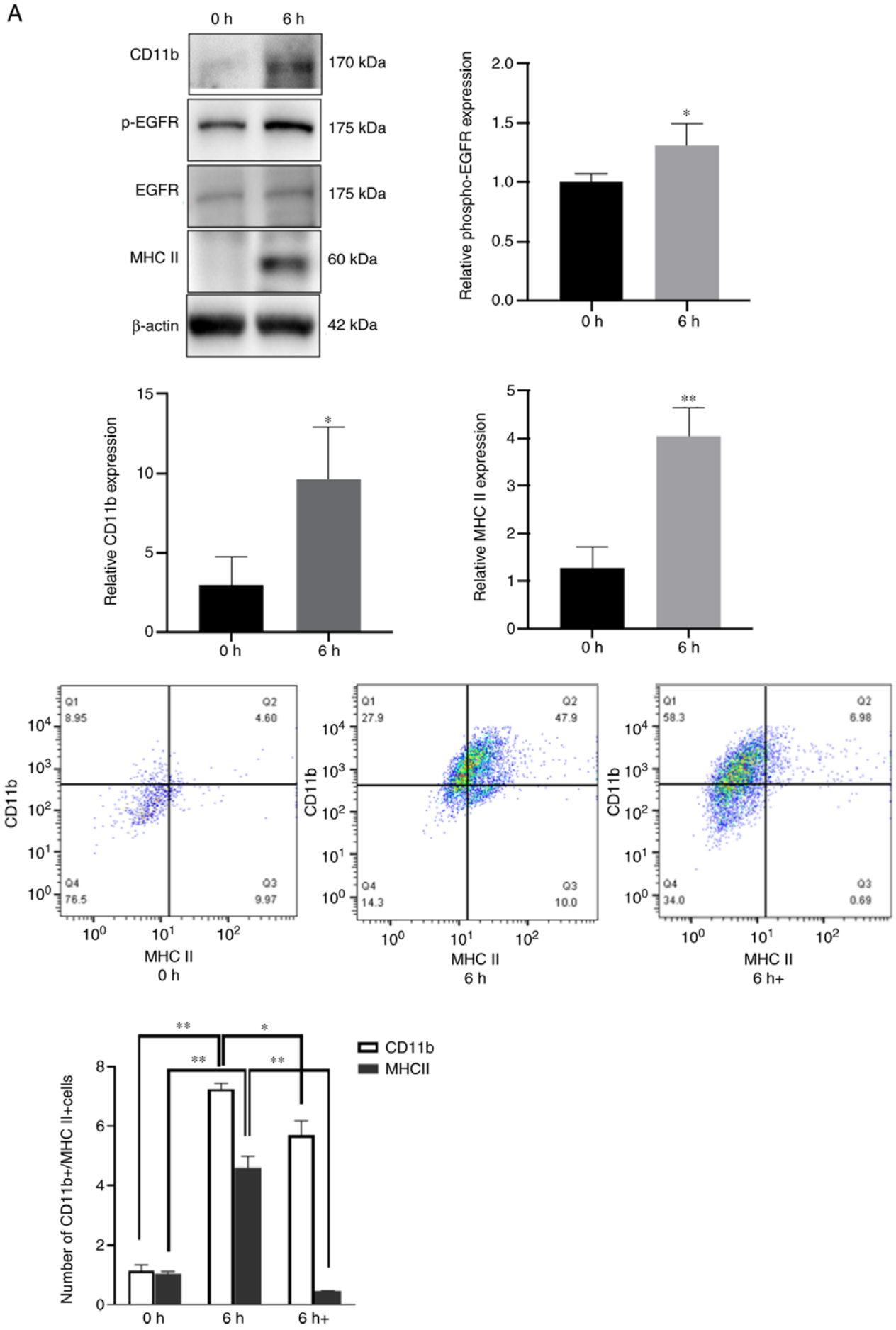

Figure 3. Continued

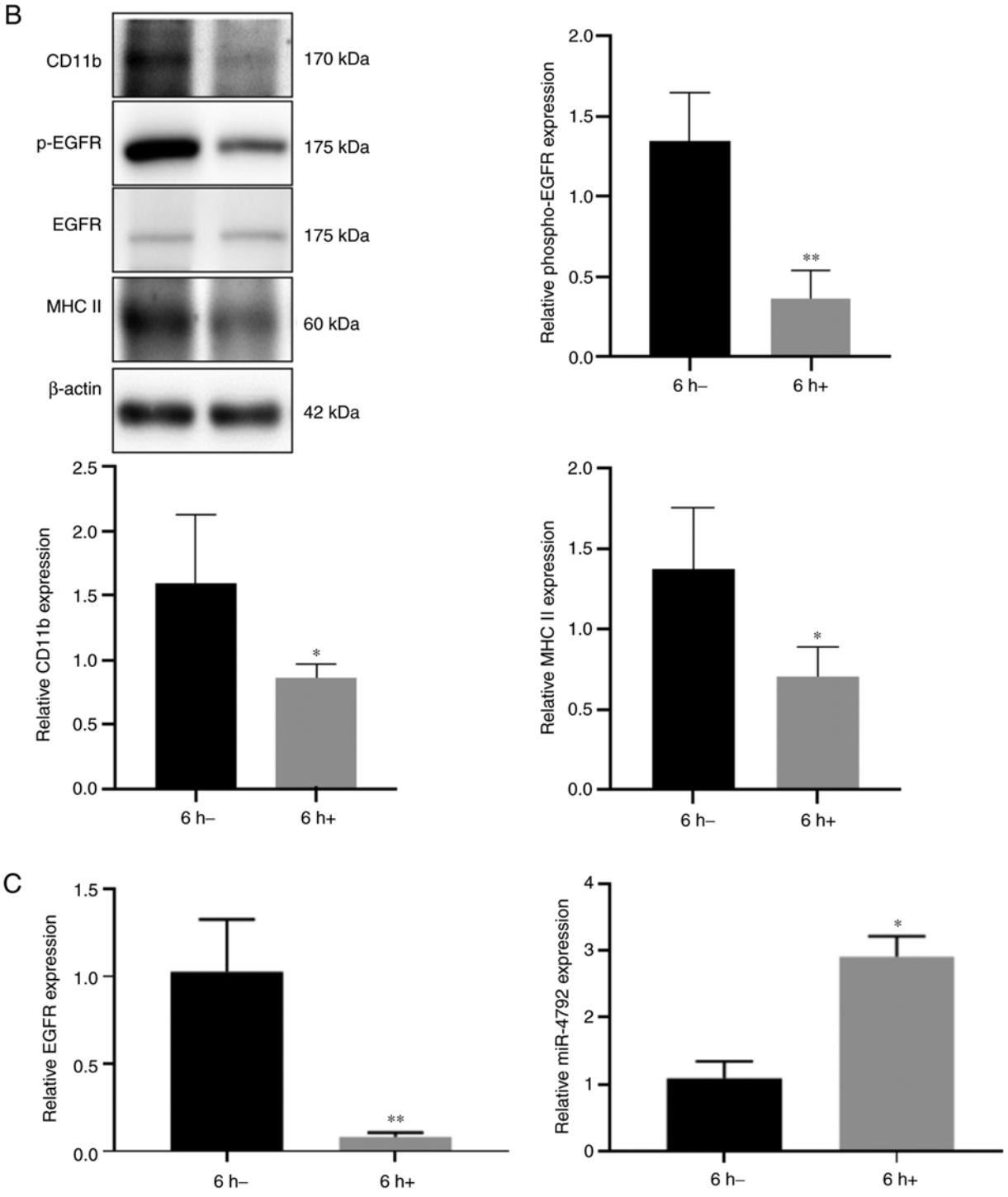

Figure 3. EGFR blockade inhibits WM148-induced microglial activation, EGFR phosphorylation and increases miR-4792 expression. Purified microglia were infected with WM148 for 6 h prior to treatment with 40 μm AG1478 for 24 h. (A) Western blot analysis of BV2 cells revealed that WM148 upregulated CD11b, MHC II and p-EGFR expression. Flow cytometry revealed that the number of $CD11b^+/MHC\ II^+$ cells increased in the presence of WM148, whereas it decreased following AG1478 stimulation. 6 h, represents BV2 cells were treated with WM148 for 6 h; 6 h+, represents BV2 cells were treated with WM148 and for 6 h and then incubated with 40 μm AG1478 for 24 h. (B) Western blot analysis showing that AG1478 suppresses CD11b, MHC II and p-EGFR expression in WM148-infected BV2 cells. (C) RT-qPCR analysis showing that AG1478 significantly suppressed EGFR expression, whilst miR-4792 expression increased. 6 h-, represents cells treated with WM148 for 6 h alone; 6 h+, represents cells treated with WM148 for 6 h and incubated with 40 μm AG1478 for 24 h. Data are the mean ± SD from three independent experiments. $^*P<0.05$; $^{**}P<0.01$, vs. the 0 h (control) or 6 h (WM148) group.

cryptococcus infection. miRNAs protect the host from infection by regulating key genes involved in host immune defenses amongst different phenotypes of macrophages and immune responses (44,45). *In vitro*, macrophage phagocytosis is directly associated with clinical outcome (46,47). As previously demonstrated, following *C. neoformans* exposure in human monocytic THP-1 cells, miR-146a is upregulated and inhibits NF-κB activation and inflammatory cytokine release (12). miRNAs function in concert to induce host defenses and are frequently dysregulated in an array of disease

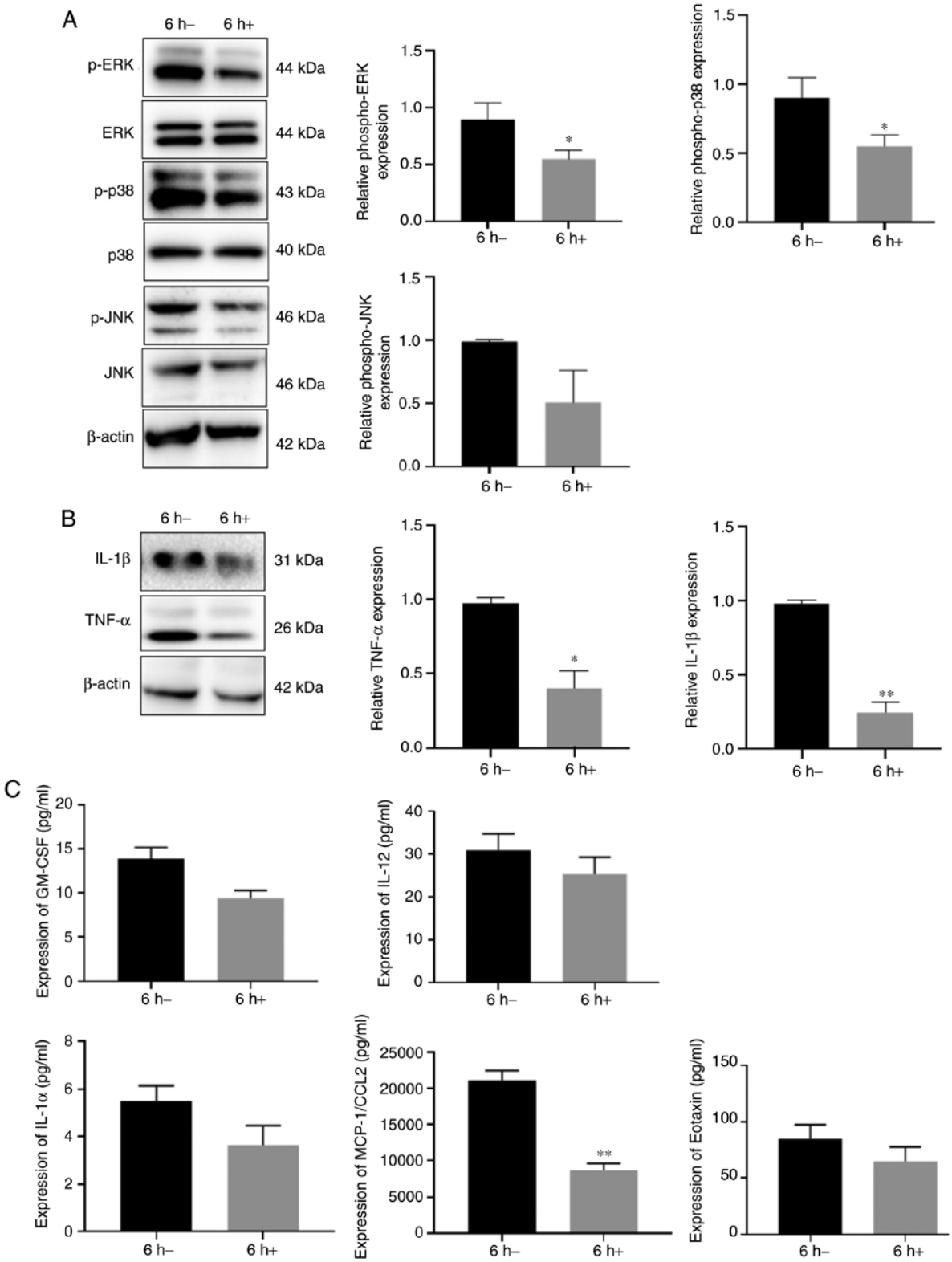

Figure 4. EGFR blockade suppresses EGFR/MAPK activation and cytokine production. BV2 cells were treated with WM148 for 6 h, followed by incubation with 40 μm AG1478 for 24 h. Western blot analysis of the phosphorylation status of ERK, JNK, p38MAPK and cytokine production (IL-1β and TNFα). 6 h-, represents cells treated with WM148 alone; 6 h+, represents cells treated with WM148 for 6 h and incubated with 40 μm AG1478 for 24 h. (A) p-ERK and p-p38 levels are significantly decreased by AG1478, whilst p-JNK levels were not significantly affected (B) Decreased expression of TNF-α and IL-1β. (C) Expression of IL-1α (P=0.13), IL-12 (P=0.29), eotaxin (P=0.25), GM-CSF (P=0.055) and MCP-1/CCL2 (P=0.009) compared to WM148 treatment, amongst which the expression of MCP-1/CCL2 significantly decreased. Data are the mean ± SD from three independent experiments. *P<0.05; **P<0.01, vs. the 6 h-group.

models (23-25,31), including following exposure to fungal pathogens. As such, miRNAs serve as novel biomarkers for fungal infections.

In the present study, in BV2 cells, exposure to WM148 led to a significant upregulation of IL-1β, TNF-α and IL-6 expression levels. Pro-inflammatory cytokines are key

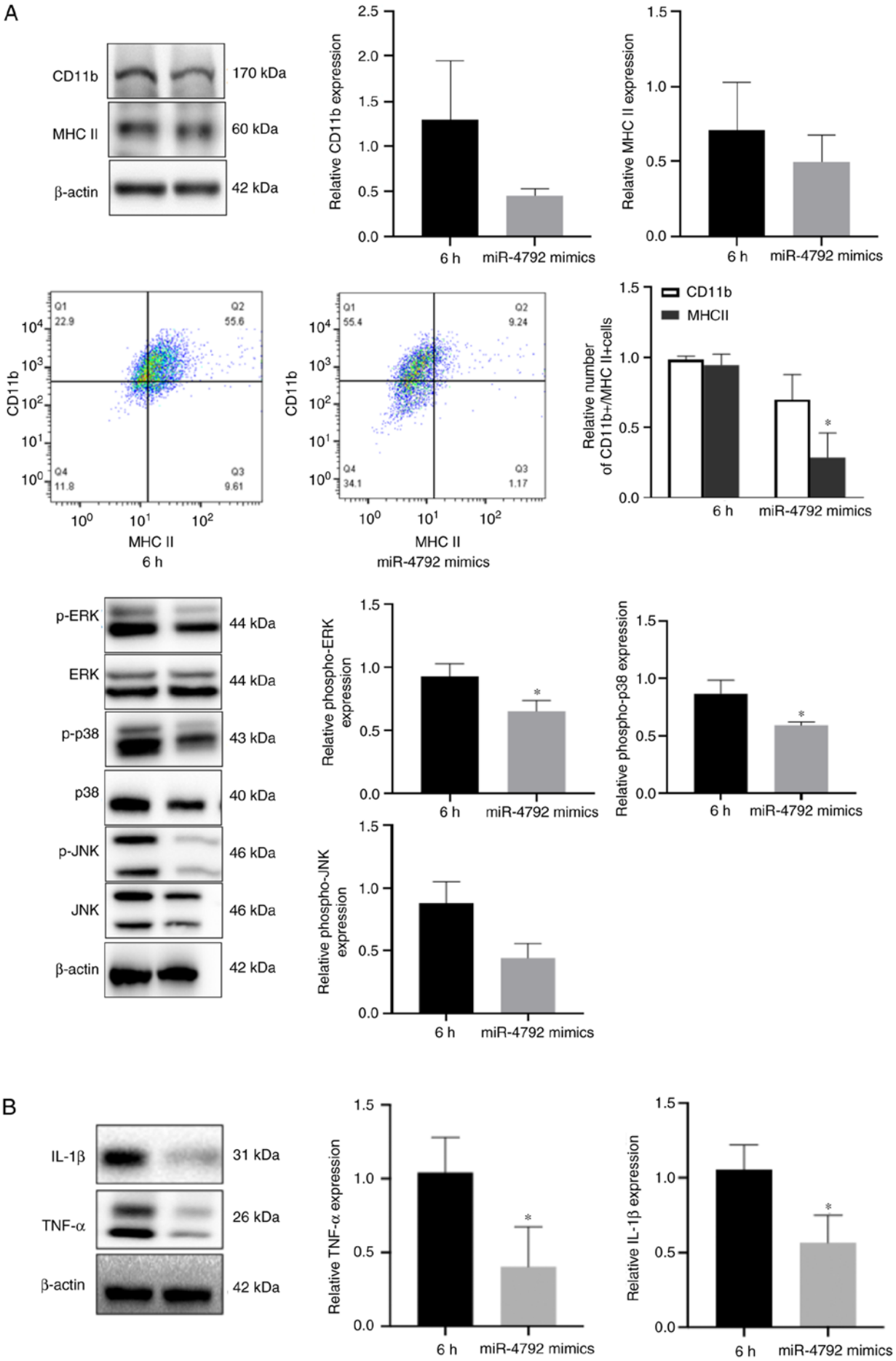

Figure 5. Continued.

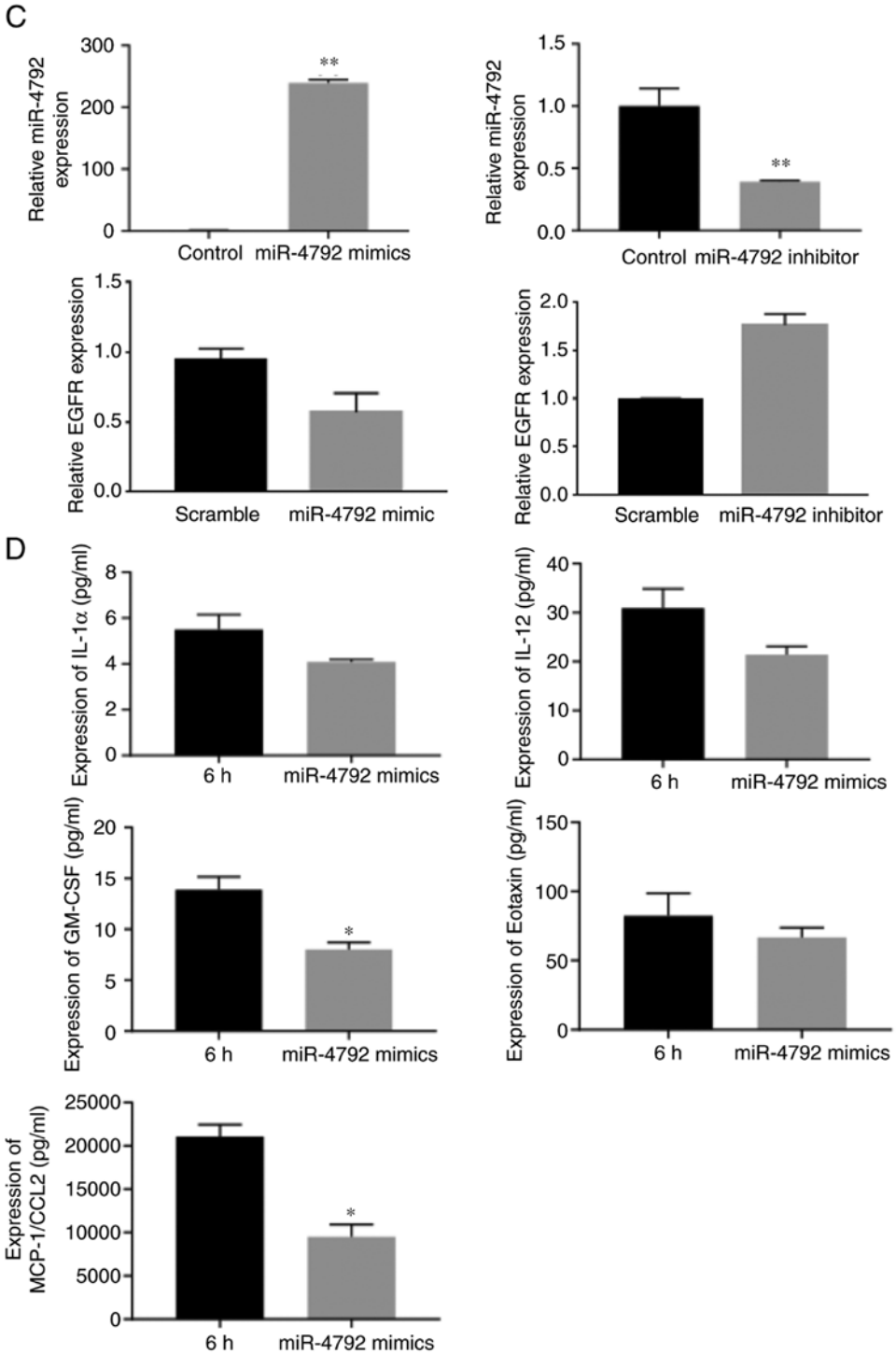

Figure 5. miR-4792 mimics suppress EGFR/MAPK activation and cytokine production. BV2 cells were treated with WM148 for 6 h, followed by incubation with 50 nM miR-4792 mimics for 24 h. Western blot analysis was performed to assess the phosphorylation status of ERK, JNK and p38 and cytokine production (IL-1β and TNFα). 6 h, treated with WM148 alone; miR-4792 mimics, transfected with WM148 for 6 h and 50 nM miR-4792 mimics for 24 h. (A) Western blot analysis of BV2 cells showing that miR-4792 mimics suppressed the phosphorylation of ERK and p38 following WM148 induction, whilst the expression of CD11b, MHC II and p-JNK exhibited no significant differences. Flow cytometry showing that the number of $CD11b^{+}$/MHC II^{+} cells decreases in the presence of miR-4792 mimics compared with the WM148 group, whilst no significant differences were observed in the CD11b levels. (B) Western blot analysis of BV2 cells showing that miR-4792 mimics suppressed the levels of the inflammatory cytokines, IL-1β and TNFα. (C) RT-qPCR confirming the effects of miR-4792 mimics/inhibitors on miR-4792 expression, whilst the expression of EGFR did not significantly differ from the control group. (D) Quantification of cytokines showing that miR-4792 mimics suppressed the expression of IL-1α (P=0.29), IL-12 (P=0.087), eotaxin (P=0.33), GM-CSF (P=0.028) and MCP-1/CCL2 (P=0.014) compared with WM148 alone, amongst which the expression of GM-CSF and MCP-1/CCL2 significantly decreased. Data are the mean ± SD from three independent experiments. *P<0.05; **P<0.01, vs. the respective control group.

mediators of neuroinflammation in a number of CNS pathologies, highlighting the ability of *C. neoformans* to induce a neuroinflammatory phenotype (32,48-50). BV2 cells are RAF/Myc immortalized murine neonatal microglia models and act as surrogates for primary microglia (51). The suitability of BV2 microglia as an alternative model system

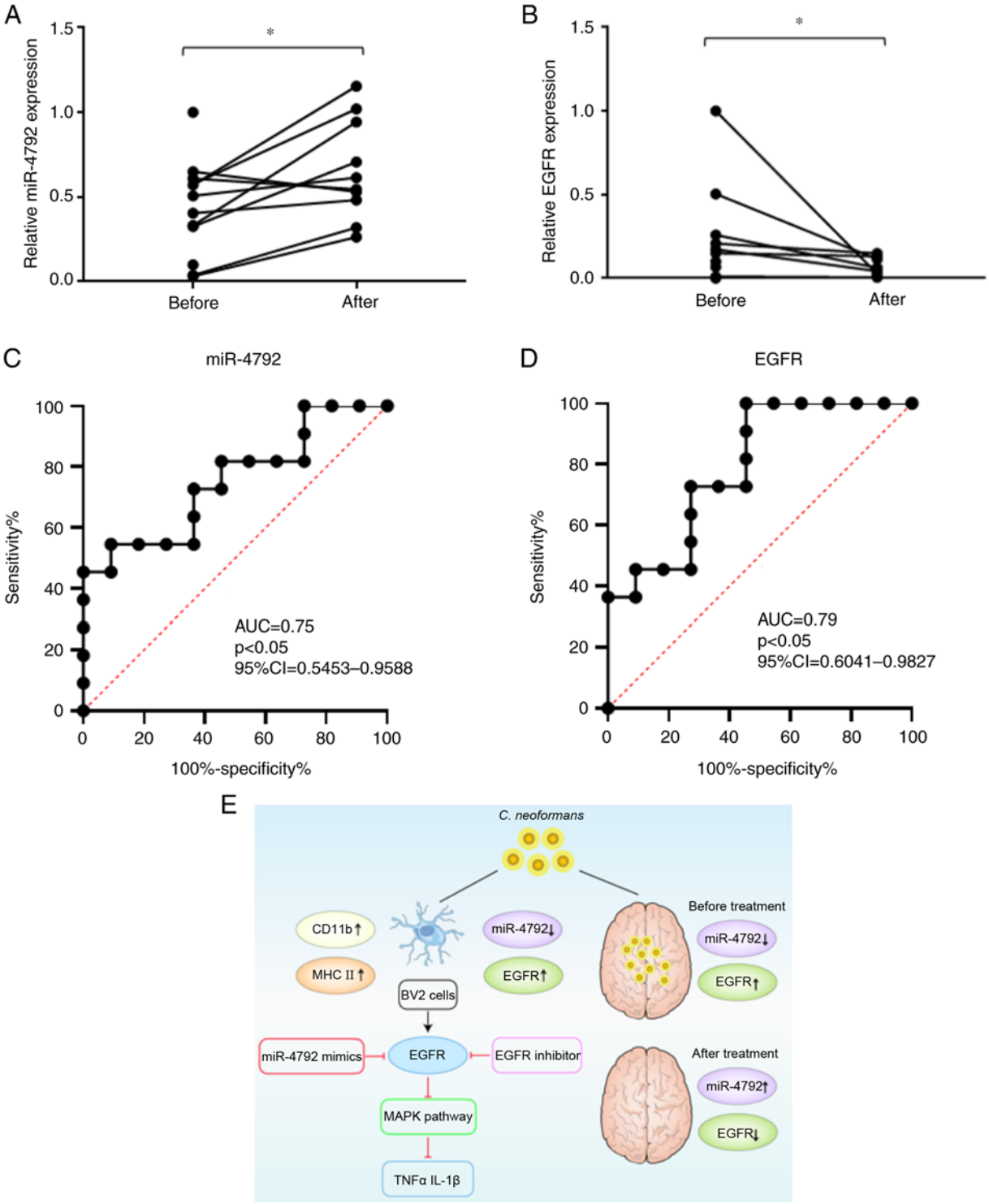

Figure 6. Expression of miR-4792 and EGFR in patients with cryptococcal meningitis before and after treatment. (A and B) qPCR showing that the expression of miR-4792 in CSF significantly increased following treatment, whilst the expression of EGFR in CSF significantly decreased following treatment. (C and D) Receiver operating characteristic (ROC) curve for CSF miR-4792 and EGFR to distinguish patients with cryptococcal meningitis before and after treatment. AUC, area under the curve; CI, confidence interval. (E) Proposed model of the regulatory and functional role for miR-4792 and EGFR in the process of *C. neoformans* infecting BV2 cells. Data are the mean ± SD of three assays. *P<0.05, vs. compared the before treatment.

has been previously established (51,52). These *in vitro* data further highlight the inflammatory responses induced by *C. neoformans*.

Neuroinflammation is the coordinated response of the CNS to threats posed by a variety of conditions, including pathogens and trauma. Responses are mediated by the production of cytokines, chemokines, reactive oxygen species and secondary messengers. These mediators are produced by resident CNS glia (microglia and astrocytes), endothelial cells and peripherally derived immune cells. Initially, inflammation is defined and determined by the release of pro-inflammatory cytokines, such as TNF-α, IL-1β and adhesion molecules. IL-1β and TNF-α play

an integral role in pathological inflammation and the acceleration of disease (49). Microglia are key effector cells in the host defense to microbial infections and act as antigen presenting cells that can produce active substances that promote inflammatory cell death (53,54). Following *C. neoformans* exposure, microglia produce TNF-α, IL-1β and IL-6 to upregulate MHC class II and CD11c expression (55,56). Moreover, microglia can phagocytose *C. neoformans* and upregulate inducible nitric oxide synthase (iNOS) levels with anti-fungal effects that are dependent on G protein-coupled receptor 43 (GPR43) expression (57-60). Despite the phagocytic capabilities of microglia, they are unable to destroy yeast cells and remain susceptible to latent intracellular infections (60,61). Microglia are also activated in response to injury in which cell-surface CD11b is a typical phenotypic marker (35). Microglia continually survey the microenvironment for noxious agents and injury, and respond to extracellular signals to clear debris and toxic substances, and secret trophic factors, providing neuroprotection. Increasing evidence implicates microglial activation as a major cause of CNS inflammation, the suppression of which reduces tissue damage and morphological alterations (62-64). This highlights microglia as critical for analysis during *C. neoformans* infection.

In the present study, the role for EGFR/MAPK signaling in WM148-mediated inflammation in the CNS was confirmed. EGFR is expressed in astrocytes, neurons oligodendrocytes and microglia (65,66). The inhibition of EGFR/MAPK signaling prevents microglial inflammatory responses by attenuating Ras/Raf/MAPK signaling (65). MAPK activation is essential for the production of inflammatory cytokines, including IL-1β, TNF-α and IL-6, and regulates cell survival, differentiation and proliferation through its effects on gene expression (37,67). Oral epithelial cells infected with *Candida albicans* activate three MAPK subfamilies and enhance the production of inflammatory mediators (68). *Sporothrix schenckii* yeast induces the robust activation of JNK, ERK1/2 and p38 MAPK in dendritic cells, which is related to IL-6 and TNF-α secretion (69). Recent study demonstrated that miR-4792 participates in the apoptotic induction of A549 cells through RTHF via the MAPK pathway and determines the apoptotic mechanism (70). In the present study, it was found that miR-4792 mimics/inhibitors did not significantly influence EGFR expression at the transcript level, suggestive of translational regulation. It was found that the inhibition of EGFR led to the inhibition of downstream MAPK signaling, preventing microglial activation and inflammatory cytokine production. Taken together, these data highlight the importance of EGFR and its effects on MAPK signaling and pro-inflammatory factors during the microglial inflammatory response to *C. neoformans*.

Exposure to dangerous pathogenic fungal infections poses a risk to human health. Enhancing the current understanding of the mechanisms governing the host innate immune response to pathogenic infections can lead to the discovery of novel anti-fungal agents. Previous studies have solely focused on the endpoint of the host response to fungal exposure (68,69); however, the specific molecular mechanisms underlying these responses differ for fungal species. Although an array of studies has investigated the pulmonary immunological response following both chronic and acute exposure to lethal fungal spores (71-73), the miRNAs that mediate these responses/deficiencies are poorly characterized. In the present study, using up-to-date models and the assessment of miR-4792 and EGFR in clinical samples, the role of miR-4792 and EGFR in the host immune response to fungal exposure was specifically analyzed. The data provide a theoretical basis for the future development of anti-fungal immune therapeutic regimens and permit the identification of at-risk populations, enabling targeted treatments to those deemed most at risk, providing a novel methodology for the assessment of the treatment efficacy for patients with CM. Following effective treatment, the expression of miR-4792 CSF increases, whilst EGFR expression decreases, which can be used as an effective index to judge whether patients can be discharged from hospital. However, the present study had certain limitations. For example, human primary microglia are difficult to culture *in vitro*; thus, BV2 cells were used as an alternative. As miRNAs are highly conserved, the results may guide future human assessments. Further studies on the role of miR-4792 in cryptococcal meningitis animal models are required however, through its intramedullary injection using liposomes or exosomes.

Acknowledgements

Not applicable.

Funding

The present study was supported by the National Natural Science Foundation of China (NSFC; grant no. 81772158).

Availability of data and materials

The datasets used and/or analyzed during the current study are available from the corresponding author on reasonable request.

Authors' contributions

JC, ZW and YJ designed the present study. GY, XW and YaW performed the experiments. QH, RG and LT analyzed the data and prepared the figures. GY and YiW drafted the initial manuscript. YiW, ZW and WL discussed and interpreted the results, commented on the manuscript and revised the manuscript. GY and JC confirm the authenticity of all the raw data. All authors have read and approved the final manuscript.

Ethics approval and consent to participate

The present study was approved by the Ethics Committee of Changzheng Hospital and written consent was obtained from all patients.

Patient consent for publication

Not applicable.

Competing interests

The authors declare that they have no competing interests.

References

1. Pappas PG: Cryptococcal infections in non-HIV-infected patients. Trans Am Clin Climatol Assoc 124: 61-79, 2013.
2. Rajasingham R, Smith RM, Park BJ, Jarvis JN, Govender NP, Chiller TM, Denning DW, Loyse A and Boulware DR: Global burden of disease of HIV-associated cryptococcal meningitis: An updated analysis. Lancet Infect Dis 17: 873-881, 2017.
3. Wu B, Liu H, Huang J, Zhang W and Zhang T: Pulmonary cryptococcosis in non-AIDS patients. Clin Invest Med 32: E70-E77, 2009.
4. Kishi K, Homma S, Kurosaki A, Kohno T, Motoi N and Yoshimura K: Clinical features and high-resolution CT findings of pulmonary cryptococcosis in non-AIDS patients. Respir Med 100: 807-812, 2006.
5. Chang YC, Stins MF, McCaffery MJ, Miller GF, Pare DR, Dam T, Paul-Satyaseela M, Kim KS and Kwon-Chung KJ: Cryptococcal yeast cells invade the central nervous system via transcellular penetration of the blood-brain barrier. Infect Immun 72: 4985-4995, 2004.
6. Ngamskulrungroj P, Chang Y, Sionov E and Kwon-Chung KJ: The primary target organ of *Cryptococcus gattii* is different from that of *Cryptococcus neoformans* in a murine model. mBio 3: e00103-e00112, 2012.
7. Chang YC, Bien CM, Lee H, Espenshade PJ and Kwon-Chung KJ: Sre1p, a regulator of oxygen sensing and sterol homeostasis, is required for virulence in *Cryptococcus neoformans*. Mol Microbiol 64: 614-629, 2007.
8. Ribes S, Ebert S, Regen T, Agarwal A, Tauber SC, Czesnik D, Spreer A, Bunkowski S, Eiffert H, Hanisch UK, *et al*: Toll-like receptor stimulation enhances phagocytosis and intracellular killing of nonencapsulated and encapsulated Streptococcus pneumoniae by murine microglia. Infect Immun 78: 865-871, 2010.
9. Redlich S, Ribes S, Schütze S, Eiffert H and Nau R: Toll-like receptor stimulation increases phagocytosis of *Cryptococcus neoformans* by microglial cells. J Neuroinflammation 10: 71, 2013.
10. Gebert L and MacRae IJ: Regulation of microRNA function in animals. Nat Rev Mol Cell Biol 20: 21-37, 2019.
11. Rupaimoole R and Frank J: Slack MicroRNA therapeutics: Towards a new era for the management of cancer and other diseases. Nat Rev Drug Discov 16: 203-222, 2017.
12. Chen H, Jin Y, Chen H, Liao N, Wang Y and Chen J: MicroRNA-mediated inflammatory responses induced by *Cryptococcus neoformans* are dependent on the NF-κB pathway in human monocytes. Int J Mol Med 39: 1525-1532, 2017.
13. De Lacorte Singulani J, De Fátima Da Silva J, Gullo FP, Costa MC, Fusco-Almeida AM, Enguita FJ and Mendes-Giannini MJS: Preliminary evaluation of circulating microRNAs as potential biomarkers in paracoccidioidomycosis. Biomed Rep 6: 353-357, 2017.
14. Kumar M, Ahmad T, Sharma A, Mabalirajan U, Kulshreshtha A, Agrawal A and Ghosh B: Let-7 microRNA-mediated regulation of IL-13 and allergic airway inflammation. J Allergy Clin Immunol 128: 1077-1085, 2011.
15. Essandoh K, Li Y, Huo J and Fan GC: miRNA-mediated macrophage polarization and its potential role in the regulation of inflammatory response. Shock 46: 122-131, 2016.
16. Nahid MA, Yao B, Dominguez-Gutierrez PR, Kesavalu L, Satoh M and Chan EK: Regulation of TLR2-mediated tolerance and cross-tolerance through IRAK4 modulation by miR-132 and miR-212. J Immunol 190: 1250-1263, 2013.
17. Testa U, Pelosi E, Castelli G and Labbaye C: miR-146 and miR-155: two key modulators of immune response and tumor development. Noncoding RNA 3: 22, 201.
18. Li Y and Chen X: miR-4792 inhibits epithelial-mesenchymal transition and invasion in nasopharyngeal carcinoma by targeting FOXC1. Biochem Biophys Res Commun 468: 863-869, 2015.
19. Georgieva B, Milev I, Minkov I, Dimitrova I, Bradford AP and Baev V: Characterization of the uterine leiomyoma microRNAome by deep sequencing. Genomics 99: 275-281, 2012.
20. Chickooree D, Zhu K, Ram V, Wu HJ, He ZJ and Zhang S: A preliminary microarray assay of the miRNA expression signatures in buccal mucosa of oral submucous fibrosis patients. J Oral Pathol Med 45: 691-697, 2016.
21. Gabrusiewicz K, Rodriguez B, Wei J, Hashimoto Y, Healy LM, Maiti SN, Thomas G, Zhou S, Wang Q, Elakkad A, *et al*: Glioblastoma-infiltrated innate immune cells resemble M0 macrophage phenotype. JCI Insight 1: e85841, 2016.
22. Li CC, Eaton SA, Young PE, Lee M, Shuttleworth R, Humphreys DT, Grau GE, Combes V, Bebawy M, Gong J, *et al*: Glioma microvesicles carry selectively packaged coding and non-coding RNAs which alter gene expression in recipient cells. RNA Biol 10: 1333-1344, 2013.
23. Liu G, Jiang C, Li D, Wang R and Wang W: MiRNA-34a inhibits EGFR-signaling-dependent MMP7 activation in gastric cancer. Tumor Biol 35: 9801-9806, 2014.
24. Chen S, Zhang Z, Chen L and Zhang J: miRNA 101 3p.1 as an independent diagnostic biomarker aggravates chronic obstructive pulmonary disease via activation of the EGFR/PI3K/AKT signaling pathway. Mol Med Rep 20: 4293-4302, 2019.
25. Ma HP, Kong WX, Li XY, Li W, Zhang Y and Wu Y: miRNA-223 is an anticancer gene in human non-small cell lung cancer through the PI3K/AKT pathway by targeting EGFR. Oncol Rep 41: 1549-1559, 2019.
26. Williamson PR: The relentless march of cryptococcal meningitis. Lancet Infect Dis 17: 790-791, 2017.
27. Bocchini V, Mazzolla R, Barluzzi R, Blasi E, Sick P and Kettenmann H: An immortalized cell line expresses properties of activated microglial cells. J Neurosci Res 31: 616-621, 1992.
28. Sheng W, Zong Y, Mohammad A, Ajit D, Cui J, Han D, Hamilton JL, Simonyi A, Sun AY, Gu Z, *et al*: Pro-inflammatory cytokines and lipopolysaccharide induce changes in cell morphology, and upregulation of ERK1/2, iNOS and sPLA2-IIA expression in astrocytes and microglia. J Neuroinflammation 8: 121, 2011.
29. Livak KJ and Schmittgen TD: Analysis of relative gene expression data using real-time quantitative PCR and the 2(-Delta Delta C(T)) method. Methods 25: 402-408, 2001.
30. Saag MS, Graybill RJ, Larsen RA, Pappas PG, Perfect JR, Powderly WG, Sobel JD and Dismukes WE: Practice guidelines for the management of cryptococcal disease. Infectious diseases society of America. Clin Infect Dis 30: 710-718, 2000.
31. Jin Y, Yao G, Wang Y, Teng L, Wang Y, Chen H, Gao R, Lin W, Wang Z and Chen J: MiR-30c-5p mediates inflammatory responses and promotes microglia survival by targeting eIF2α during *Cryptococcus neoformans* infection. Microb Pathog 141: 103959, 2020.
32. Wang WY, Tan MS, Yu JT and Tan L: Role of pro-inflammatory cytokines released from microglia in Alzheimer's disease. Ann Transl Med 3: 136, 2015.
33. Jin X and Yamashita T: Microglia in central nervous system repair after injury. J Biochem 159: 491-496, 2016.
34. Kraft AD and Harry GJ: Features of microglia and neuroinflammation relevant to environmental exposure and neurotoxicity. Int J Environ Res Public Health 8: 2980-3018, 2011.
35. O'Sullivan JB, Ryan KM, Curtin NM, Harkin A and Connor TJ: Noradrenaline reuptake inhibitors limit neuroinflammation in rat cortex following a systemic inflammatory challenge: Implications for depression and neurodegeneration. Int J Neuropsychopharmacol 12: 687-699, 2009.
36. Loane DJ and Byrnes KR: Role of microglia in neurotrauma. Neurotherapeutics 7: 366-377, 2010.
37. Bachstetter AD, Xing B, de Almeida L, Dimayuga ER, Watterson DM and Van Eldik LJ: Microglial p38alpha MAPK is a key regulator of proinflammatory cytokine up-regulation induced by toll-like receptor (TLR) ligands or beta-amyloid (Aβ). J Neuroinflammation 8: 79, 2011.
38. Xu L, Huang Y, Yu X, Yue J, Yang N and Zuo P: The influence of p38 mitogen-activated protein kinase inhibitor on synthesis of inflammatory cytokine tumor necrosis factor alpha in spinal cord of rats with chronic constriction injury. Anesth Analg 105: 1838-1844, 2007.
39. Kim SH, Smith CJ and Van Eldik LJ: Importance of MAPK pathways for microglial pro-inflammatory cytokine IL-1 beta production. Neurobiol Aging 25: 431-439, 2004.
40. Qu WS, Tian DS, Guo ZB, Fang J, Zhang Q, Yu ZY, Xie MJ, Zhang HQ, Lü JG and Wang W: Inhibition of EGFR/MAPK signaling reduces microglial inflammatory response and the associated secondary damage in rats after spinal cord injury. J Neuroinflammation 9: 178, 2012.
41. Yamauchi T, Ueki K, Tobe K, Tamemoto H, Sekine N, Wada M, Honjo M, Takahashi M, Takahashi T, Hirai H, *et al*: Growth hormone-induced tyrosine phosphorylation of EGF receptor as an essential element leading to MAP kinase activation and gene expression. Endocr J 45 (Suppl): S27-S31, 1998.
42. Goel S, Hidalgo M and Perez-Soler R: EGFR inhibitor-mediated apoptosis in solid tumors. J Exp Ther Oncol 6: 305-320, 2007.

43. Pinheiro SB, Sousa ES, Cortez ACA, da Silva Rocha DF, Menescal LSF, Chagas VS, Gómez ASP, Cruz KS, Santos LO, Alves MJ, *et al*: Cryptococcal meningitis in non-HIV patients in the State of Amazonas, Northern Brazil. J Microbiol 52: 279-288, 2021.
44. Martinez-Nunez RT, Louafi F and Sanchez-Elsner T: The interleukin 13 (IL-13) pathway in human macrophages is modulated by microRNA-155 via direct targeting of interleukin 13 receptor alpha1 (IL13Ralpha1). J Biol Chem 286: 1786-1794, 2011.
45. Roy S: miRNA in macrophage development and function. Antioxid Redox Signal 25: 795-804, 2016.
46. Sabiiti W, Robertson E, Beale MA, Johnston SA, Brouwer AE, Loyse A, Jarvis JN, Gilbert AS, Fisher MC, Harrison TS, *et al*: Efficient phagocytosis and laccase activity affect the outcome of HIV-associated cryptococcosis. J Clin Invest 124: 2000-2008, 2014.
47. Alanio A, Desnos-Ollivier M and Dromer F: Dynamics of *Cryptococcus neoformans*-macrophage interactions reveal that fungal background influences outcome during cryptococcal meningoencephalitis in humans. mBio 2: e00158-e00111, 2011.
48. Ji RR, Nackley A, Huh Y, Terrando N and Maixner W: Neuroinflammation and central sensitization in chronic and widespread pain. Anesthesiology 129: 343-366, 2018.
49. Lyman M, Lloyd DG, Ji X, Vizcaychipi MP and Ma D: Neuroinflammation: The role and consequences. Neurosci Res 79: 1-12, 2014.
50. Kim YK, Na KS, Myint AM and Leonard BE: The role of pro-inflammatory cytokines in neuroinflammation, neurogenesis and the neuroendocrine system in major depression. Prog Neuropsychopharmacol Biol Psychiatry 64: 277-284, 2016.
51. Henn A, Lund S, Hedtjärn M, Schrattenholz A, Pörzgen P and Leist M: The suitability of BV2 cells as alternative model system for primary microglia cultures or for animal experiments examining brain inflammation. ALTEX 26: 83-94, 2009.
52. Stansley B, Post J and Hensley K: A comparative review of cell culture systems for the study of microglial biology in Alzheimer's disease. J Neuroinflammation 9: 115, 2012.
53. Kofler J and Wiley CA: Microglia: Key innate immune cells of the brain. Toxicol Pathol 39: 103-114, 2011.
54. Rock RB, Gekker G, Hu S, Sheng WS, Cheeran M, Lokensgard JR and Peterson PK: Role of microglia in central nervous system infections. Clin Microbiol Rev 17: 942-964, 2004.
55. Barluzzi R, Brozzetti A, Delfino D, Bistoni F and Blasi E: Role of the capsule in microglial cell-*Cryptococcus neoformans* interaction: Impairment of antifungal activity but not of secretory functions. Med Mycol 36: 189-197, 1998.
56. Neal LM, Xing E, Xu J, Kolbe JL, Osterholzer JJ, Segal BM, Williamson PR and Olszewski MA: CD4^{+}T cells orchestrate lethal immune pathology despite fungal clearance during *Cryptococcus neoformans* meningoencephalitis. mBio 11: e01415-e01417, 2017.
57. Adami C, Sorci G, Blasi E, Agneletti AL, Bistoni F and Donato R: S100B expression in and effects on microglia. Glia 33: 131-142, 2001.
58. Song X, Tanaka S, Cox D and Lee SC: Fc gamma receptor signaling in primary human microglia: Differential roles of PI-3K and Ras/ERK MAPK pathways in phagocytosis and chemokine induction. J Leukoc Biol 75: 1147-1155, 2004.
59. Preissler J, Grosche A, Lede V, Le Duc D, Krügel K, Matyash V, Szulzewsky F, Kallendrusch S, Immig K, Kettenmann H, *et al*: Altered microglial phagocytosis in GPR34-deficient mice. Glia 63: 206-215, 2015.
60. Lee SC, Kress Y, Dickson DW and Casadevall A: Human microglia mediate anti-*Cryptococcus neoformans* activity in the presence of specific antibody. J Neuroimmunol 62: 43-52, 1995.
61. Lee SC, Kress Y, Zhao ML, Dickson DW and Casadevall A: *Cryptococcus neoformans* survive and replicate in human microglia. Lab Invest 73: 871-879, 1995.
62. Popovich PG, Guan Z, Wei P, Huitinga I, van Rooijen N and Stokes BT: Depletion of hematogenous macrophages promotes partial hindlimb recovery and neuroanatomical repair after experimental spinal cord injury. Exp Neurol 158: 351-365, 1999.
63. Stirling DP, Khodarahmi K, Liu J, McPhail LT, McBride CB, Steeves JD, Ramer MS and Tetzlaff W: Minocycline treatment reduces delayed oligodendrocyte death, attenuates axonal dieback, and improves functional outcome after spinal cord injury. J Neurosci 24: 2182-2190, 2004.
64. Tian DS, Xie MJ, Yu ZY, Zhang Q, Wang YH, Chen B, Chen C and Wang W: Cell cycle inhibition attenuates microglia induced inflammatory response and alleviates neuronal cell death after spinal cord injury in rats. Brain Res 1135: 177-185, 2007.
65. Gomez-Pinilla F, Knauer DJ and Nieto-Sampedro M: Epidermal growth factor receptor immunoreactivity in rat brain. Development and cellular localization. Brain Res 438: 385-390, 1988.
66. Erschbamer M, Pernold K and Olson L: Inhibiting epidermal growth factor receptor improves structural, locomotor, sensory, and bladder recovery from experimental spinal cord injury. J Neurosci 27: 6428-6435, 2007.
67. Jung HW, Son HY, Minh CV, Kim YH and Park YK: Methanol extract of ficus leaf inhibits the production of nitric oxide and proinflammatory cytokines in LPS-stimulated microglia via the MAPK pathway. Phytother Res 22: 1064-1069, 2008.
68. Correia I, Prieto D, Román E, Wilson D, Hube B, Alonso-Monge R and Pla J: Cooperative role of MAPK pathways in the interaction of *Candida albicans* with the host epithelium. Microorganisms 25: 48, 2019.
69. Uenotsuchi T, Takeuchi S, Matsuda T, Urabe K, Koga T, Uchi H, Nakahara T, Fukagawa S, Kawasaki M, Kajiwara H, *et al*: Differential induction of Th1-prone immunity by human dendritic cells activated with sporothrix schenckii of cutaneous and visceral origins to determine their different virulence. Int Immunol 18: 1637-1646, 2006.
70. Liu P, Pu J, Zhang J, Chen Z, Wei K and Shi L: Bioinformatic analysis of mir-4792 regulates *Radix Tetrastigma hemsleyani* flavone to inhibit proliferation, invasion, and induce apoptosis of a549 cells. Onco Targets Ther 12: 1401-1412, 2019.
71. Lindell DM, Ballinger MN, McDonald RA, Toews GB and Huffnagle GB: Immunologic homeostasis during infection: coexistence of strong pulmonary cell-mediated immunity to secondary *Cryptococcus neoformans* infection while the primary infection still persists at low levels in the lungs. J Immunol 177: 4652-4661, 2006.
72. Lindell DM, Ballinger MN, McDonald RA, Toews GB and Huffnagle GB: Diversity of the T-cell response to pulmonary *Cryptococcus neoformans* infection. Infect Immun 74: 4538-4548, 2006.
73. Eastman AJ, Osterholzer JJ and Olszewski MA: Role of dendritic cell-pathogen interactions in the immune response to pulmonary cryptococcal infection. Future Microbiol 10: 1837-1857, 2015.